

Coupling GA with SVM for feature selection in high-resolution remote sensing target recognition

SUN Ning¹, CHEN Qiuxiao¹, LUO Jiancheng², SHEN Zhanfeng², HU Xiaodong²

1. Institute of Urban Planning Engineering and Information Technology, Zhejiang University, Zhejiang Hangzhou 310058, China;

2. Institute of Remote Sensing Applications, Chinese Academy of Sciences, Beijing 100101, China

Abstract: As one of the key techniques for high-resolution remote sensing target recognition, feature selection focused on how to find the critical features in the feature set to represent the target. Generally, the classical methods for feature selection were as follows, principal component analysis, empirical method, etc. When using these classical methods, recognition accuracy was not guaranteed. In this paper, a new method was proposed, the main idea of which was to couple GA (Genetic Algorithm) and SVM (Support Vector Machine) for feature selection, and using recognition results to guide the revolution direction of GA. Meanwhile, to reduce the risk of premature convergence of the traditional GA, some modification had been made. The experiment demonstrated the effectiveness of the proposed method.

Key words: genetic algorithm, support vector machine, target recognition, feature selection

CLC number: TP751.1 **Document code:** A

Citation format: Sun N, Chen Q X, Luo J C, Shen Z F and Hu X D. 2010. Coupling GA with SVM for feature selection in high-resolution remote sensing target recognition. *Journal of Remote Sensing*. 14(5): 928—943

1 INTRODUCTION

The main task of remotely sensed target recognition (Ming *et al.*, 2005) (RSTR) is to determine whether interesting targets exist or not, and to find out what is the target and where it is. Mainly focusing on recognition of artificial geo-objects, RSTR relies on not only targets' spectral features and shape index, but also their spatial semantic relations with surrounding geo-objects. Generally, the main purpose of RSTR is to recognize small-scale geo-objects, and high spatial resolution aerial images and satellite images are often utilized as data source (Li *et al.*, 2006). Since the advent of remote sensing technology in the sixties of last century, RSTR has always been a hot topic in this field. In recent years, there are many researches conducted on target recognition of artificial geo-objects like building, road and bridge from remotely sensed imagery. However, how to improve the accuracy of these researches remains to be solved.

Generally speaking, RSTR includes the following three stages: image processing (including image segmentation), feature extraction, classification and recognition. As to feature extraction, spectral features, shape index and texture features are commonly used. Due to the multiband property of remotely sensed images, hundreds of features can be extracted from them if needed. However, positive features correlation will result in

redundancy and increase the computation cost of recognition respectively, while negative correlation may lead to a strange phenomenon—more features, lower accuracy. To recognize different kinds of targets, different combination of features are used. However, too much features are not necessary for recognition, and will probably reduce the recognition accuracy. That is why feature selection—finding a small number of key features from the feature set to well represent target, becomes one of the most important topic of RSTR researches (Niu & Ni, 2005; Zhang *et al.*, 2005).

At present, the empirical approach or principal component analysis are always used to find the best combination of features for target representation. However, such combination of features are not capable of distinguishing targets from non-targets, recognition accuracy is therefore not guaranteed. In consideration of the facts stated above, we proposed a coupling method named GA-SVM (coupling GA with SVM) for feature selection, through which, a small number of key features were selected. By inputting these features into classifier, building targets can be recognized from quickbird images. The experimental results showed that this method can improve recognition accuracy obviously.

2 COUPLING OF GA AND SVM

GA is a probabilistic search algorithm based on the principle

Received: 2009-08-13; **Accepted:** 2009-12-24

Foundation: “863” project (No. 2009AA12Z121, No. 2009AA12Z148), Fundamental Research Funds for the Central Universities.

First author biography: SUN Ning (1985—), female, graduate student, her research interest includes urban remote sensing and urban planning. E-mail: ningning8533@zju.edu.cn

Corresponding author: CHEN Qiuxiao, E-mail: chen_qiuxiao@zju.edu.cn

of biological evolution—the survival of the fittest, which was initially proposed by Holland (Holland, 1973, 1975) in the early 1970s. In pattern recognition domain, GA is famous for its strong robustness and adaptability, and is often used to solve complex optimization problems. However, GA does not have the ability to calculate the optimal direction. Due to the fact that recognition accuracy mainly relies on the classification results, it will be very helpful to feature selection and recognition accuracy improvement subsequently if GA is coupled with a good classifier such as SVM. SVM uses a hypothetical space of linear functions in a high dimensional feature space trained with a learning algorithm based on optimization theory. The advantage of SVM is as follows, robustness, good learning abilities and suitability for high dimensional data classification (Xu & Li, 2004; Zhang, 1997). In this paper, GA and SVM were coupled for feature selection (coupling structure shown in Fig. 1), that is to use genetic mechanism of GA to find a subset of features, construct the fitness function by the classification accuracy using SVM, and recognize all targets through SVM classifier by utilizing the optimized subset of features once they were obtained. Specifically, the coupling is reflected in the following three stages: feature dimensionality reduction, fitness calculation and target recognition.

2.1 Feature dimensionality reduction phase

In this paper, GA's population evolution was used to reduce the dimension, then vectors with reduced dimension were put into SVM and mapped to the new linear feature space, through which feature dimensionality reduction in GA and feature space mapping in SVM were combined.

$$\begin{aligned} x = (x_1, \dots, x_n) &\xrightarrow{\text{GA}} (x_1, \dots, x_d) \\ &\xrightarrow{\text{SVM}} \phi(x) = (\phi_1(x), \dots, \phi_d(x)) \quad d < n \end{aligned} \quad (1)$$

2.2 Fitness calculation phase

To improve SVM classifier's discrimination between different objects and the recognition accuracy for specific target, training sample set (S_{trn}) as well as testing sample set (S_{test}) were utilized. S_{trn} should include different types geo-objects and each sample should be representative. S_{test} consists of two categories, objects to be identified and the other ones. Because of the complexity of remote sensing images, an appropriate increase in the number of samples can be considered to improve recognition accuracy.

S_{trn} was trained in the new feature space in order to find the hyperplane that can classify S_{trn} correctly, then this hyperplane was used to classify S_{test} . By returning the fitness based on classification results to GA, the next evolution direction was well guided. Thus, the final obtained feature subset being the best combination of features for target recognition was ensured.

Here, SVM uses the following decision function:

$$f(x) = \text{sgn} \left(\sum_{i=1}^d \alpha_i y_i K(x_i, x) + b \right) \quad (2)$$

where, $K(x_i, x)$ is the Kernel function.

2.3 Results of genetic identification phase

When the population met the convergence conditions, individual with the highest fitness was outputted, feature information from the individual was read and mapped to a linear

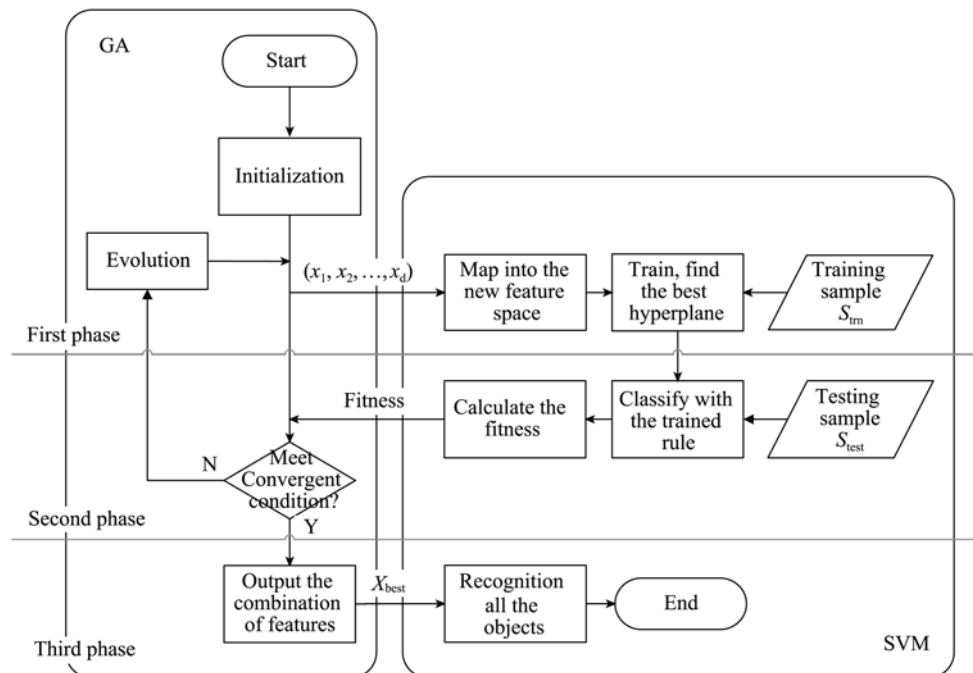


Fig. 1 Structure diagram of how to couple GA with SVM

feature space to recognize all targets, and recognition results were obtained finally.

3 IMPROVEMENT OF GA

GA is a global random optimization algorithm by simulating the species evolution. It uses binary-coded chromosome to form the population, controls the genetic process through operators like mutation and crossover. To ensure GA's reasonable evolution direction, the fitness function and convergent condition were set. On the premise of maximizing the accuracy of RSTR, the fewer features used, the better. In order to achieve this goal, the coupling of GA and SVM should not only guarantee the genetic direction to improve the recognition accuracy, but also avoid the risk of premature convergence the traditional GA brings. Therefore, some improvement on traditional GA was made by introducing the individual optimization of the selection mechanism and foreign individuals' access mechanism, and the final recognition accuracy was controlled or affected by the fitness function and population reset mechanism.

3.1 Individual choice

Individual is the basic unit that carries feature information in the genetic process. The heterogeneity and fitness of the individual in the same generation is the key factor that determines whether the final feature scheme is the best one. In order to ensure the diversity of the highest fitness of the population, Individual optimization and the foreign individual access mechanism were applied for individual selection based on binomics.

3.1.1 Individual optimization of the selection mechanism

In the population initialization phase, in order to reduce feature dimension obviously, the various components of chromosomes were randomly set to 1 with a small probability. To optimize the genetic process, reduce the possibility falling into a local minimum during the evolution, the chromosome was evaluated in the initialization process. If its fitness is less than a certain threshold value, then a new chromosome was re-generated to replace the old one.

During the genetic process, optimal string retention strategy was applied to ensure that the highest fitness of individual was directly passed to the next generation. Meanwhile, according to the individual fitness, a number of individuals were selected by the expectation selection mechanism to form the breeding herd, among which, two parents were selected randomly to complete the hybridization. Single-dot blot hybridization was used, that is, breakpoint was randomly selected, and two parts of the parents were exchanged to form new individuals. For two parents x_1, x_2 , and two offspring x_3, x_4 , fitness was calculated according to Eq. (4). Then, individual x_i with the highest fitness was found, hamming distance between x_i and other three individuals were computed in order to find x_k that had the greatest distance to x_i , x_i and x_k were then passed into the next generation.

3.1.2 Foreign individual access mechanism

To avoid local individual homogenization phenomena after

several times of evolution, foreign individual was introduced. The probability of all individuals was calculated according to Eq. (3), where $F(x)$ was the fitness obtained by Eq. (4), fit_{\max} was the largest population fitness, and fit_{\min} was the smallest one.

$$p_m(x) = \frac{\text{fit}_{\max} - F(x)}{\text{fit}_{\max} - \text{fit}_{\min}} \quad (3)$$

Based on the above probability, an individual was randomly selected and then deleted from the population, and a new one was re-initialized and added. To ensure the overall population quality, the foreign individual's fitness should be larger than 0.4.

3.2 Accuracy control

The ultimate goal of feature optimization is to improve the recognition accuracy. So, based on accuracy evolution, a fitness function was constructed by coupling GA with SVM, and population reset mechanism was introduced for convergence judgment in order to escape from the local minimum state.

3.2.1 Construction of the fitness function

To meet target recognition request, the fitness function was constructed based on recognition error and feature dimension of the training sample set:

$$F(x) = w_1 \times (1 - E_{\text{miss}}(x) - E_{\text{error}}(x)) + w_2 \times (1 - (d(x) - d_{\min}) / (d_{\max} - d_{\min})) \quad (4)$$

where, $E_{\text{miss}}(x)$ is the proportion of missed targets, $E_{\text{error}}(x)$ is the proportion of misclassified targets, $d(x)$ is the number of dimensions the chromosome contains, d_{\max} is the maximum number of dimensions x may contain, while d_{\min} is the minimum number. w_1 and w_2 correspond to the weights of target recognition accuracy and feature dimension respectively, where $w_1 + w_2 = 1$.

3.2.2 Convergence condition and population reset mechanism

Three kinds of convergence conditions are set in the algorithm: the individual's largest fitness is greater than 0.95, and this fitness has not been improved during five generations; the individual's largest fitness is greater than 0.9, and this fitness has not been improved during ten generations; algorithm has reached 100 generation evolution.

If the individual's largest fitness has not been improved during ten generations, and this fitness is smaller than 0.9, it can be assumed that the algorithm falls into a local minimum state. In such situation, population reset mechanism should be launched, the individual with the largest fitness in the generation was kept, other individuals were randomly retained, the remaining individuals was reset by initialization process, then the genetic process was restarted.

4 BUILDING TARGET RECOGNITION EXPERIMENTS IN HIGH-RESOLUTION REMOTE SENSING IMAGE

4.1 Experimental data and platform

Two subset of Quickbird image covering part of Wu'han

City were selected as experimental data, which consisted of four bands – blue, green, red and near-infrared band with spatial resolution as 0.6 meters. The sizes of test images are 1600×1600 and 1200×800 respectively. The experimental platform used in this paper was SINCE2008 developed by the Institute of Remote Sensing Application, Chinese Academy of Sciences.

4.2 Feature extraction

At the very beginning, test images were segmented by mean shift algorithm in the proper scale. In this experiment, when the scale (minimum region size) was 100 or 200 pixels, building primitives can be segmented well. For more details on Mean Shift algorithm, one can refer to (Comaniciu & Meer, 2002). Segmentation results, with 3236 and 1435 image objects respectively (Table 1), were used as input data of the classifier. Including spectral features, geometric features and texture features from the original data, 31 features were extracted. Quick-bird images used in this experiment include four bands. With the increase of the number of image bands, the number or the weight of geometrical features can be increased to avoid the decrease of the contribution of the geometric features to the final recognition results.

Table 1 Feature list

	Feature name	Feature number
Spectral features	Mean brightness	4
	Standard deviation of brightness	4
	Subtotal	8
Texture features	ASM	4
	IDM	4
	Entropy	4
	Contrast	4
	Subtotal	16
	Geometric features	Perimeter
Area		1
Bounding rectangle width		1
Bounding rectangle length		1
Bounding rectangle's principal direction		1
Shape index		1
Compactness		1
Subtotal		7
Total		31

Spectral features' computation was omitted because of its simplicity. Based on gray - gradient co-occurrence matrix, the following texture features were extracted:

$$\text{Inverse difference moment: IDM} = \sum_{i=0}^{n-1} \sum_{j=0}^{n-1} \frac{P_{ij}}{1+(i-j)^2}$$

$$\text{Angular second moment: ASM} = \sum_{i=0}^{n-1} \sum_{j=0}^{n-1} P_{ij}^2$$

$$\text{Entropy: Entropy} = \sum_{i=0}^{n-1} \sum_{j=0}^{n-1} P_{ij} \log P_{ij}$$

$$\text{Contrast: Contrast} = \sum_{i=0}^{n-1} \sum_{j=0}^{n-1} (i-j)^2 P_{ij}$$

where, $P_{ij} = C_{ij} / \sum_i \sum_j C_{ij}$, and C_{ij} was the element (i, j) of the co-occurrence matrix C . Gradient image was obtained through the following method: $g_c = \left| \sum_{i=1}^4 p_c - p_{n_i} \right|$, where p_c was the spectral value of the center pixel, p_{n_i} was that of its four neighborhood pixel.

The main geometric features were calculated as follows:

$$\text{Compactness: Compact} = 2 \times \sqrt{\pi \times \text{area}} / \text{perim}$$

$$\text{Shape Factor: ShapeIndex} = 0.25 \times \text{perim} / \sqrt{\text{area}}$$

4.3 Experimental samples and experimental parameters' specification

The training sample set and test sample set were selected separately (Table 2). For two test images, the former had 276 and 256 objects respectively, which were put into four categories (building, shadow, green, road), while the latter 537 objects and 365 objects respectively, which were put into two categories (building and non-building).

Table 2 Sample set

Training sample set		
Categories name	Object number	
	1st image	2nd image
Building	67	78
Shadow	63	34
Green	77	87
Road	69	57
Test sample set		
Categories name	Object number	
	1st image	2nd image
Building	123	110
Non-building	414	255

GA's parameters were set as follows: population size was 50; in initialization phrase, each chromosome was set to 1 with a probability of 0.3; the weight of target recognition accuracy (w_1) was set to 0.9 since the ultimate goal was to maximize the target recognition accuracy.

Because of the uncertainty of GA, and in consideration that different order of features may lead to a different result, the experiment had been conducted for 20 times using the same data, and the average results were utilized for evaluation of the performance of the proposed coupling method (GA-SVM).

As to SVM algorithm, third-order Gaussian kernel function was used, the value of s parameters and c parameters were 1.0 in simmoid function, the epsilon in loss function of epsilon-SVR was set to 0.9, c -parameter of epsilon-SVR 25, and threshold for terminating training 0.01. The process of coupling GA and SVM methods is shown in Fig. 2 and Fig. 3).

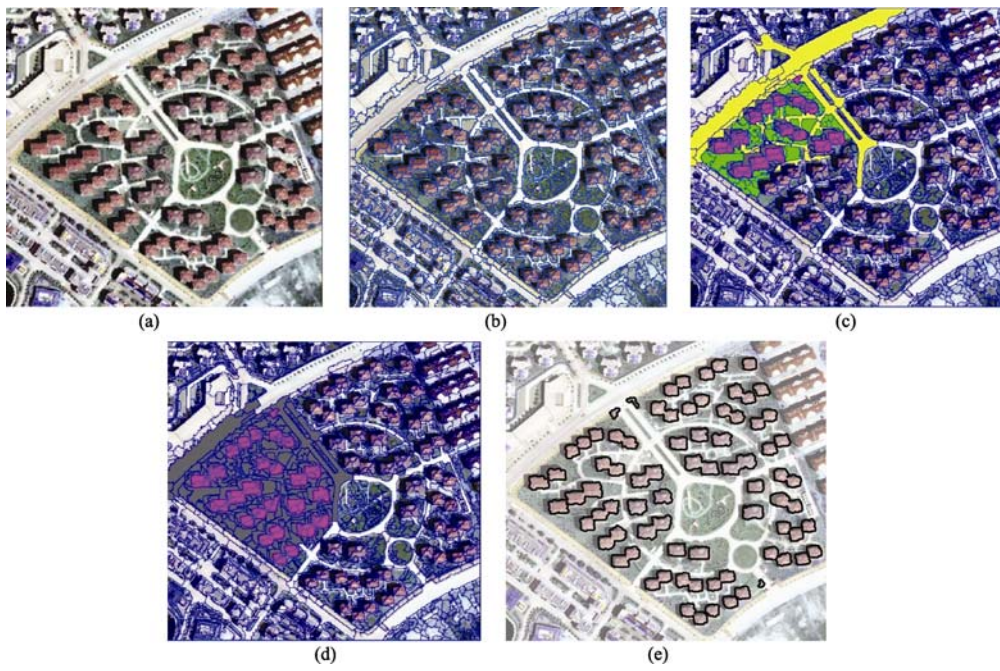


Fig. 2 Building recognition process using the coupling method GA-SVM (I)

(a) 1st Quickbird test image; (b) Segmentation results; (c) Training sample set; (d) Test sample set; (e) Building recognition results with the highest accuracy

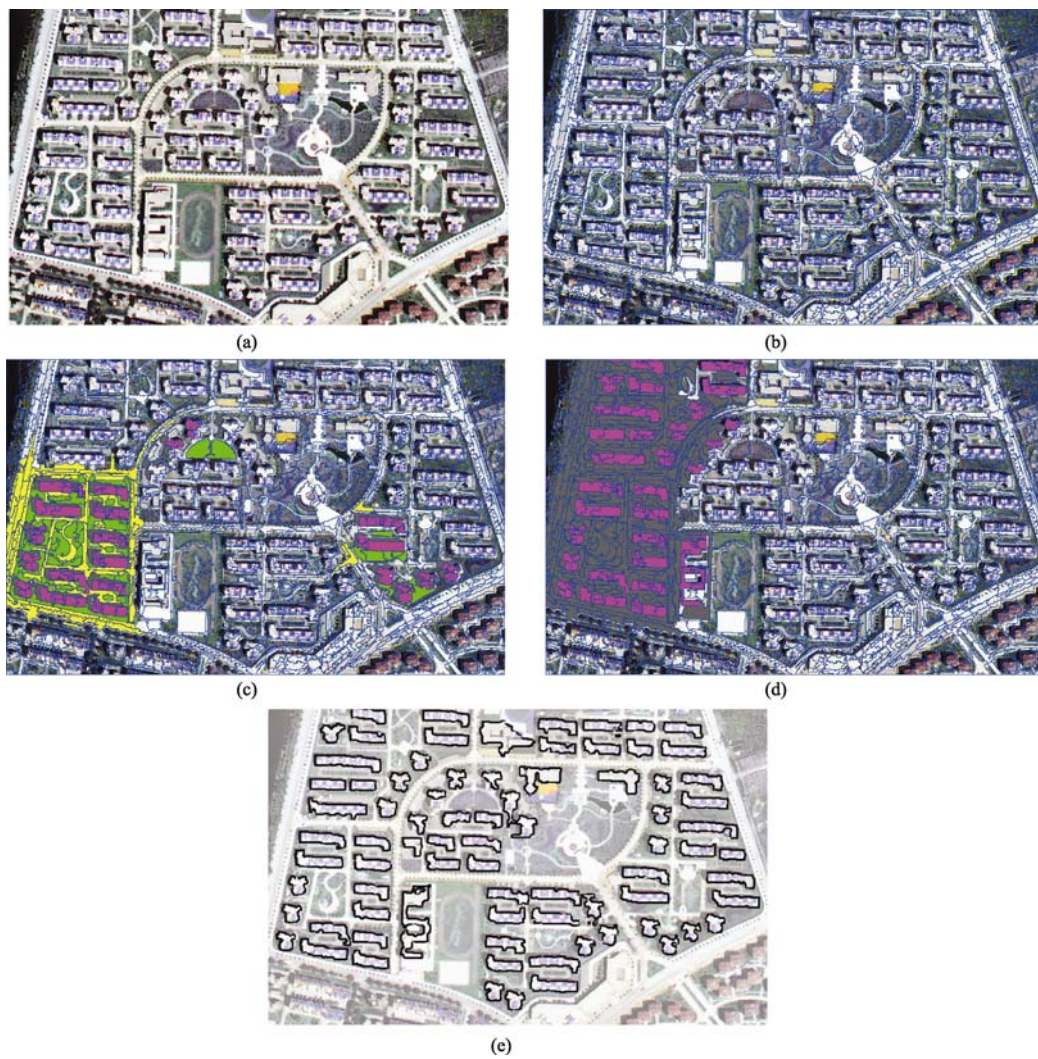


Fig. 3 Building recognition process using the coupling method GA-SVM ()

(a) 2nd Quickbird test image; (b) Segmentation results; (c) Training sample set; (d) Test sample set; (e) Building recognition results with the highest accuracy

4.4 Methods for comparison and some relevant specification

To verify the effectiveness of the proposed method, the following methods were used for comparison: (1) GA coupled with minimum distance classifier; (2) PCA (principle component analysis) method; classical GA coupled with SVM; (3) empirical method. For PCA, the principal components extracted should at least represent 95% of original data information. The difference between (3) and the proposed method was as follows, the former did not use the individual optimization of the selection mechanism, the foreign individual access mechanism, and the population reset mechanism as well. Except (1), all methods utilized SVM as classifier.

4.5 Experimental results and analysis

Experimental results Table 3 and Table 4 showed that for two test images the optimal feature subset obtained from the proposed method contains averagely 9.65 and 8.25 features respectively, common features that all 20 times experiments outputted were listed in Fig. 4 (b) and Fig. 5 (b) respectively, recognition accuracy varied from 98.48% to 96.59%, and from 93.31% to 90.66% respectively, with an average accuracy as 97.86% and 92.24%, the standard deviation as 0.41% and

0.64% accordingly. From the above results, we can learn that our proposed method was a robust one with high accuracy at least for building recognition. The result are shown in Table 5 and Table 6.

Comparison of the proposed GA-SVM method with classical ones was shown in Table 7. From this table, we note that recognition accuracy was quite low—from 50.76% to 68.08% while using all the features. This number was slightly higher when utilizing PCA for feature dimension reduction. Because of the presence of premature convergence effect, and the relative homogeneous characteristic of targets, the classical GA method did not have an obvious advantage over the empirical method (using spectral features by experience). Comparing methods listed in Table 3 and Table 4, we can learn that by utilizing the proposed method recognition accuracy was improved significantly. When coupling GA with the minimum distance classifier, the recognition accuracy was lower compared with the proposed GA-SVM method, which means that SVM is a good classifier for coupling. In addition, the proposed one outperformed the method by coupling classical GA with SVM because the improved GA (used in the former) can always guide GA's evolution direction towards the improvement of target recognition accuracy, and reduce its risk of premature convergence as well.

Table 3 Final recognition accuracy and corresponding feature number of twenty experiments (1st test image)

Experiment No.	1st	2nd	3rd	4th	5th	6th	7th	8th	9th	10th
Optimal features number	11	9	9	12	12	11	10	8	9	8
Recognition accuracy/%	97.73	97.73	98.30	98.48	98.11	98.11	98.11	97.73	97.73	98.30
Experiment No.	11th	12th	13th	14th	15th	16th	17th	18th	19th	20th
Optimal features number	8	10	6	10	10	11	10	8	12	9
Recognition accuracy/%	97.54	98.30	96.59	97.54	97.54	97.54	98.11	97.73	98.11	97.92

Table 4 Final recognition accuracy and corresponding feature number of twenty experiments (2nd test image)

Experiment No.	1st	2nd	3rd	4th	5th	6th	7th	8th	9th	10th
Optimal features number	9	12	8	8	9	10	7	8	7	12
Recognition accuracy/%	93.03	92.68	92.61	92.20	93.17	92.13	91.99	91.50	93.17	93.31
Experiment No.	11th	12th	13th	14th	15th	16th	17th	18th	19th	20th
Optimal features number	6	7	9	9	6	9	10	4	8	7
Recognition accuracy/%	91.64	92.20	91.57	92.47	92.61	92.06	91.92	91.78	92.13	90.66

Mean Britness_Band1	Mean Britness_Band1
Mean Britness_Band2	Mean Britness_Band2
Mean Britness_Band3	Mean Britness_Band3
Mean Britness_Band4	Mean Britness_Band4
AREA	AREA
ASM_Band1	ASM_Band1
ASM_Band1	
IDM_Band3	
IDM_Band4	
ENTROPY_Band1	
ENTROPY_Band3	
CONTRAST_Band3	

(a)

(b)

Mean Britness_Band1	Mean Britness_Band1
Mean Britness_Band2	Mean Britness_Band2
Mean Britness_Band3	Mean Britness_Band3
Principal Direction	Principal Direction
Compactness	Compactness
AMS_Band1	AMS_Band1
AMS_Band2	CONTRAST_Band2
AMS_Band3	
AMS_Band4	
ENTROPY_Band3	
CONTRAST_Band2	
CONTRAST_Band3	

(a)

(b)

Fig. 4 Feature selection result of 1st test image

(a) Feature list with the highest accuracy; (b) Features included in over 10 experiments results

Fig. 5 Feature selection result of 2nd test image

(a) Feature list with the highest accuracy; (b) Features included in over 10 experiments results

Table 5 List of selected features in each experiment using 1st test image

Experiment No.	1	2	3	4	5	6	7	8	9	10	11	12	13	14	15	16	17	18	19	20
Mean brightness_Band1	⊙	⊙	⊙	⊙	⊙	⊙	⊙	⊙	⊙	⊙	⊙	⊙	⊙	⊙	⊙	⊙	⊙	⊙	⊙	⊙
Mean brightness_Band2	⊙	⊙	⊙	⊙	⊙	⊙	⊙	⊙	⊙	⊙	⊙	⊙	⊙	⊙	⊙	⊙	⊙	⊙	⊙	⊙
Mean brightness_Band3	⊙	⊙	⊙	⊙	⊙	⊙	⊙	⊙	⊙	⊙	⊙	⊙	⊙	⊙	⊙	⊙	⊙	⊙	⊙	⊙
Mean brightness_Band4	⊙	⊙	⊙	⊙	⊙	⊙	⊙		⊙		⊙	⊙				⊙		⊙		⊙
Standard deviation of brightness_Band1	⊙		⊙																	
Standard deviation of brightness_Band2	⊙				⊙															
Standard deviation of brightness_Band3					⊙															
Standard deviation of brightness_Band4																				
Perimeter										⊙										
Area	⊙	⊙	⊙	⊙	⊙	⊙	⊙		⊙				⊙	⊙	⊙	⊙	⊙		⊙	
Bounding rectangle width																				
Bounding rectangle length					⊙															
Bounding rectangle's principal direction		⊙							⊙	⊙		⊙								⊙
Shape index		⊙					⊙							⊙					⊙	
Compactness													⊙					⊙		
ASM_Band1	⊙	⊙	⊙	⊙	⊙	⊙		⊙			⊙	⊙	⊙	⊙	⊙	⊙				
ASM_Band2				⊙		⊙		⊙							⊙		⊙		⊙	
ASM_Band3	⊙		⊙			⊙		⊙									⊙		⊙	
ASM_Band4						⊙		⊙						⊙					⊙	
IDM_Band1							⊙	⊙		⊙	⊙			⊙			⊙	⊙		⊙
IDM_Band2	⊙										⊙									
IDM_Band3		⊙		⊙			⊙		⊙				⊙			⊙		⊙		
IDM_Band4				⊙				⊙											⊙	⊙
ENTROPY_Band1			⊙	⊙	⊙	⊙	⊙									⊙	⊙			⊙
ENTROPY_Band2					⊙						⊙	⊙			⊙					⊙
ENTROPY_Band3				⊙					⊙					⊙	⊙				⊙	
ENTROPY_Band4							⊙													⊙
CONTRAST_Band1											⊙							⊙		
CONTRAST_Band2						⊙				⊙		⊙				⊙	⊙		⊙	⊙
CONTRAST_Band3				⊙	⊙							⊙		⊙	⊙	⊙				
CONTRAST_Band4	⊙					⊙	⊙		⊙					⊙		⊙		⊙		

⊙ denotes the feature is selected in the corresponding experiment.

Table 6 List of selected features in each experiment using 2nd test image

Experiment No.	1	2	3	4	5	6	7	8	9	10	11	12	13	14	15	16	17	18	19	20
Mean brightness_Band1	⊙	⊙	⊙	⊙	⊙	⊙	⊙	⊙	⊙	⊙	⊙	⊙	⊙	⊙	⊙	⊙	⊙	⊙	⊙	⊙
Mean brightness_Band2	⊙	⊙	⊙	⊙	⊙	⊙	⊙	⊙	⊙	⊙	⊙	⊙	⊙	⊙	⊙	⊙	⊙	⊙	⊙	⊙
Mean brightness_Band3	⊙	⊙	⊙	⊙	⊙	⊙	⊙	⊙	⊙	⊙	⊙	⊙	⊙	⊙	⊙	⊙	⊙	⊙	⊙	⊙
Mean brightness_Band4																				
Standard deviation of brightness_Band1																				
Standard deviation of brightness_Band2																				
Standard deviation of brightness_Band3																				
Standard deviation of brightness_Band4									⊙											
Perimeter												⊙								
Area	⊙				⊙		⊙							⊙						
Bounding rectangle width																				
Bounding rectangle length																				
Bounding rectangle's principal direction		⊙	⊙	⊙	⊙	⊙		⊙		⊙						⊙	⊙			
Shape index			⊙										⊙	⊙					⊙	⊙
Compactness	⊙				⊙			⊙		⊙	⊙		⊙		⊙	⊙	⊙		⊙	
ASM_Band1				⊙		⊙	⊙	⊙	⊙	⊙		⊙	⊙		⊙		⊙	⊙		
ASM_Band2		⊙				⊙				⊙			⊙							
ASM_Band3									⊙	⊙	⊙					⊙				
ASM_Band4				⊙	⊙	⊙								⊙						
IDM_Band1	⊙	⊙										⊙		⊙		⊙				
IDM_Band2	⊙					⊙											⊙			⊙
IDM_Band3													⊙	⊙						
IDM_Band4		⊙	⊙	⊙						⊙							⊙		⊙	
ENTROPY_Band1														⊙						
ENTROPY_Band2		⊙	⊙		⊙														⊙	
ENTROPY_Band3				⊙						⊙			⊙					⊙		
ENTROPY_Band4							⊙										⊙			
CONTRAST_Band1		⊙							⊙						⊙					
CONTRAST_Band2	⊙	⊙		⊙		⊙		⊙		⊙						⊙	⊙		⊙	⊙
CONTRAST_Band3		⊙						⊙		⊙	⊙									⊙
CONTRAST_Band4	⊙	⊙		⊙	⊙									⊙						

⊙ denotes the feature is selected in the corresponding experiment.

Table 7 Comparison of GA-SVM and other feature selection methods

Feature selection method	1st test image				2nd test image			
	Undetected	Wrong detected	Error rate	Accuracy	Undetected	Wrong detected	Error rate	Accuracy
Empirical method (using spectral features by experience)	3.03	9.85	12.88	87.12	3.76	6.97	10.73	89.27
No selection (using all features)	46.21	3.03	49.24	50.76	11.92	20.00	31.92	68.08
Principle component analysis	11.36	26.52	37.88	62.12	8.36	12.26	20.63	79.37
Classical GA coupled with SVM	3.03	11.36	14.39	85.61	2.72	6.62	9.34	90.66
GA-SVM	0.00	1.52	1.52	98.48	2.72	3.97	6.69	93.31
GA coupled with minimum distance classifier	9.45	11.74	21.19	78.81	7.69	6.76	14.45	85.55

5 CONCLUSION AND DISCUSSION

In this paper, a feature optimization method was proposed for target recognition from high spatial resolution remote sensing images. Experimental results showed that the proposed method, having obvious advantages compared with other feature selection methods, can effectively reduce the dimension of feature space, and improve target recognition accuracy. Besides, some modification had been made to improve the classical GA. Thus, the risk of premature convergence of GA had been reduced greatly, and better genetic evolution results can be obtained.

It should be pointed out that, the above experiments only chose quickbird data as the test image, and the building type in the test image were relatively simple. So, how to improve the universality of the proposed GA-SVM method so that it can be applied to other type of high-resolution remotely sensed imagery, and how to successfully recognize different type of buildings from the image will be further studied in the near future.

REFERENCES

- Chen G L and Wang X F. 1999. Genetic Algorithm and Its Application. Beijing: Posts & Telecom Press
- Comaniciu D, Meer P. 2002. Mean shift: a robust approach toward feature space analysis. *IEEE Trans. on Pattern Analysis and Machine Intelligence*, **24**(5): 603—619
- He A X, Zhu Y H and An K. 2007. Tumor molecular classification based on genetic algorithms and support vector machines. *Journal of Data Acquisition & Processing*, **22**(1): 84—89
- Holland J H. 1973. Genetic algorithms and the optimal allocations of trials. *SIAM Journal of Computing*, **2**: 88—105
- Holland J H. 1975. Adaptation in Natural and Artificial System. Ann Arbor: The University of Michigan Press
- Li J M, Hu Y H and Chen X Q. 2006. Feature optimizing expert system for pattern recognition. *Electronics Optics&Control*, **13**(1): 20—26
- Ming D P, Luo J C, Shen Z F, Wang M and Sheng H. 2005. Research on information extraction and target recognition from high resolution remote sensing image. *Science of Surveying and Mapping*, **30**(3): 18—20
- Niu L H and Ni G Q. 2005. Feature optimization for multi_sensor target recognition system. *Optical Technique*, **31**(3): 420—426
- Nello C and John S T. 2004. An Introduction to Support Vector Machines and Other Kernel-based Learning Methods. Cambridge: Cambridge University Press
- Vapnik V N. 1998. Statistical learning theory. New York: Wiley Interscience
- Xu J Q and Li G P. 2004. Feature selection for SVM based on genetic algorithm. *Computer Engineering*, **30**(24): 1—2, 182
- Zhang X H. 1997. Genetic algorithms and its application. *Fire Control & Command Control*, **22**(4): 49—53
- Zhang Y B and Zhang Q. 2005. Support vector machine for classification of remotely sensed image. *Geospatial Information*, **3**(4): 24—26

面向遥感目标识别耦合 GA 与 SVM 的特征优选方法

孙 宁¹, 陈秋晓¹, 骆剑承², 沈占锋², 胡晓东²

1. 浙江大学 城市规划工程与信息技术研究所, 浙江 杭州 310058;

2. 中国科学院 遥感应用研究所, 北京 100101

摘 要: 提出了 GA-SVM 耦合用于高分遥感目标识别的特征优选方法, 将 GA 中的特征降维和适应度函数构建与 SVM 中的特征空间映射、样本训练以及分类结果在内容上耦合, 利用 SVM 的识别结果指导 GA 的进化方向。同时, 为减小未成熟收敛风险, 对传统 GA 做了改进。实验表明, 该方法在高分遥感影像目标识别中效果较好。

关键词: 遗传算法, 支持向量机, 目标识别, 特征优选

中图分类号: TP751.1

文献标志码: A

引用格式: 孙 宁, 陈秋晓, 骆剑承, 沈占锋, 胡晓东. 2010. 面向遥感目标识别耦合 GA 与 SVM 的特征优选方法. 遥感学报, 14(5): 928—943

Sun N, Chen Q X, Luo J C, Shen Z F and Hu X D. 2010. Coupling GA with SVM for feature selection in high-resolution remote sensing target recognition. *Journal of Remote Sensing*. 14(5): 928—943

1 引 言

遥感目标识别(明冬萍等, 2005)的主要任务是确定遥感影像中是否存在感兴趣的目标, 并给目标以合理的解释, 即判断目标是什么并确定它(们)的位置。遥感影像目标识别一般针对人工地物进行, 不仅依据其光谱特征、还很大程度上依据目标形状、空间语义关系等, 其落脚点往往是小尺度的目标类别归属, 一般其数据源为高空间分辨率的航空影像和卫星影像(李军梅等, 2006)。自 20 世纪 60 年代遥感技术问世以来, 遥感目标识别技术一直是遥感研究领域的热点。近年来, 针对建筑物、道路、桥梁等人工地物的遥感目标识别研究方兴未艾。但是如何提高该类研究的识别精度仍然是有待解决的难题。

遥感影像目标识别一般包括 3 个阶段: 影像处理(包括影像分割)、特征提取和分类识别。其中, 特征提取是目标识别的关键。通常认为, 描述遥感影像的特征有光谱特征、纹理特征、结构特征和形状特征。由于遥感影像通常是多波段影像, 可以藉此

提取几十乃至上百个影像特征。但是, 特征间普遍存在的相关性(正相关)将造成特征冗余, 增加识别时的计算开销; 而特征间的负相关可能导致特征越多精度越低的现象。不同地物目标的提取对应于不同的最优特征组合, 过多的冗余特征会降低识别方法的性能, 减弱目标识别与提取效果。为提高识别精度, 如何进行特征优选——即从众多的特征中找到最能反映待识别目标特性的少量关键特征, 在保证识别精度的同时, 提高识别的效率, 便成为遥感目标识别研究的一项重要内容(牛丽红 & 倪国强, 2005; 张耀波 & 张迁, 2005)。

目前, 高分辨率遥感影像目标识别过程中通常是根据经验提取最优特征组合, 或用主成分分析法进行降维, 由于这些特征并不一定能表达目标区分于非目标的本质特性, 因而识别精度难以保证。基于以上考虑, 本文提出并使用一种耦合 GA 和 SVM 的特征优选方法来提取用以描述待识别目标的最优特征组合, 利用该特征组合识别 Quickbird 影像中的建筑物目标。实验结果表明, 该特征优选方法明显地提高了目标识别的精度。

收稿日期: 2009-08-13; 修订日期: 2009-12-24

基金项目: 863 项目(编号: 2009AA12Z121, 2009AA12Z148)及中央高校基本科研业务费专项资金。

第一作者简介: 孙 宁(1985—), 女, 硕士研究生, 研究方向为城市规划和城市遥感。E-mail: ningning8533@zju.edu.cn。

通讯作者: 陈秋晓, E-mail: chen_qiuxiao@zju.edu.cn。

2 耦合 GA 和 SVM 的特征优选方法

遗传算法(genetic algorithm, GA)(陈国良 & 王煦法, 1999)是 Holland(Holland, 1973, 1975)于 20 世纪 70 年代初创建的一种概率搜索算法, 体现了优胜劣汰、适者生存的生物进化原理。在模式识别的解决上具有较强的鲁棒性和自适应性, 常用解决复杂的优化问题。然而, GA 本身并不具备计算最优方向的能力, 由于目标识别的精度主要是依靠分类结果进行评价的, 需要将 GA 与一个优秀的分类器如支持向量机结合以进一步优选特征并提高识别精度(何爱香等, 2007)。支持向量机(support vector machine, SVM)是在高维特征空间使用线性函数假设空间的学习系统(Nello & John, 2004; Vapnik, 1998), 具有较强的稳健性和学习能力, 在处理高维数据的分类上有优势(许建强 & 李高平, 2004; 章新华, 1997)。本文将 GA 与 SVM 方法进行耦合(图 1), 通过 GA 的遗传机制从候选特征集中选择满足条件的最优组合, 利用 SVM 算法构建 GA 中的适应度函数, 使用 GA 优选出的最优特征组合识别全体对象。具体地, 耦合体现在以下 3 个阶段: 特征降维、适应度计算、目标识别。

2.1 特征降维阶段

原 N 维特征空间是非线性空间, 本文将 GA 的

特征降维与 SVM 的特征空间映射相结合, 利用 GA 的种群进化对原 N 维特征向量实现降维, 将降维后的特征向量传入 SVM 分类器并映射到新的线性特征空间。

$$x = (x_1, \dots, x_n) \xrightarrow{\text{GA}} (x_1, \dots, x_d) \xrightarrow{\text{SVM}} \phi(x) = (\phi_1(x), \dots, \phi_d(x)) \quad d < n \quad (1)$$

2.2 适应度计算阶段

为提高不同地物间的区分度, 同时提高分类模型对特定地物的识别精度, 本文为分类器选择两类样本集, 训练样本集 S_{trn} 和测试样本集 S_{test} 。训练样本集要能反映数据的各种类型并且有代表性; 测试样本集分两类, 分别为待识别目标和非待识别目标。由于高分遥感影像类型复杂, 数据量大, 考虑适当增加样本数以提高识别精度。在新的特征空间中对训练样本集 S_{trn} 进行训练, 寻找能够将训练样本集正确分类的最优超平面。本文的支撑向量机采用如下的决策函数:

$$f(x) = \text{sgn} \left(\sum_{i=1}^d \alpha_i y_i K(x_i, x) + b \right) \quad (2)$$

式中, $K(x_i, x)$ 为核函数。

利用训练后规则分类测试样本集 S_{test} , 依据该结果计算适应度反馈回 GA, 指导下一回的进化方向, 从而保证最终得到的特征子集为该目标识别的最优特征组合。

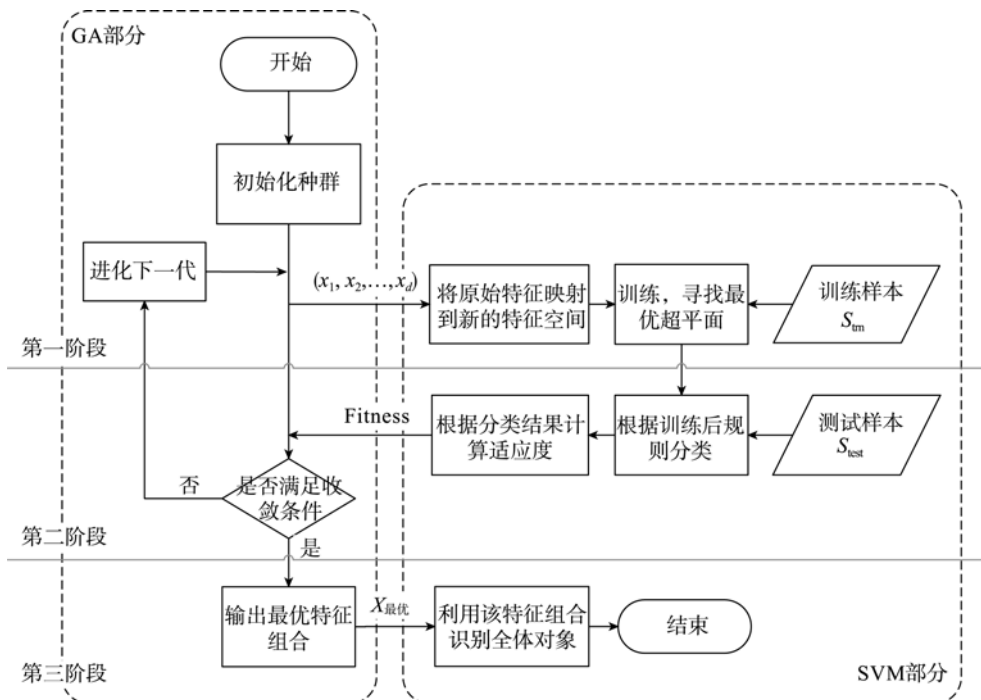


图 1 GA 与 SVM 耦合结构图

2.3 遗传结果识别阶段

当种群满足收敛条件后, 输出适应度最高个体, 从个体中读取特征信息, 将该特征子集映射到 SVM 的线性特征空间中对全体对象进行识别, 得到最终识别结果。

3 遗传算法改良

遗传算法是一种模拟生物界进化的全局随机优化算法, 它利用二进制编码染色体组成遗传种群, 通过三类算子控制遗传过程, 并设置适应度函数和收敛条件保证 GA 的遗传向最优化发展。高分辨率遥感目标识别要求特征方案中应包含尽可能少又有针对性的特征, 能够最大限度的提高最终识别精度。这就要求 GA-SVM 既能够保证遗传向提高识别精度方向发展, 又能改善传统 GA 带来的未成熟收敛的风险, 针对该特性本文在 GA-SVM 耦合算法中对传统 GA 进行了一些改进, 添加了个体优化选择机制和外来个体进入机制, 通过适应度函数和种群重置机制的构建控制最终识别精度。

3.1 个体选择

遗传个体是遗传操作中携带特征信息的基本单位, 同一代遗传个体的异质性和适应度是决定最终获得特征方案是否最优的重要因素。为保证群体的多样化, 提高群体最高适应度, 本文依据仿生学原理, 在个体选择中添加个体优化选择机制和外来个体准入机制。

3.1.1 个体优化选择机制

在群体初始化阶段, 由于待选特征集较大, 为达到显著降维的目的, 初始化时以较小的概率将染色体的各分量随机设置为 1。为优化遗传进程, 减少在进化过程中陷入局部极小的概率, 在初始化过程中对染色体进行判断, 若适应度小于一定阈值, 则重新生成染色体。

在遗传过程中, 附加最优串保留策略, 保留适应度最高的个体直接进入下一代。同时, 根据个体的适应度, 用期望值选择机制从上一代中选择用于繁殖的若干个体组成繁殖群, 然后从繁殖群中随机选择两父代进行杂交。杂交选择单点杂交的方式, 即随机选择断点, 在断点处交换两父代的尾部形成新的个体。对两父代 x_1 、 x_2 , 以及两子代 x_3 、 x_4 , 根据式(4)计算适应度, 找到适应度最高的个体 x_i , 对 x_i 与其他 3 个个体计算汉明距离, 找到距离最大的 x_k , 将 x_i 和 x_k 进入下一代。

3.1.2 外来个体准入机制

为抑制本地个体在经历多次进化后产生的同质化现象, 在进化中引入外来个体。根据式(3)对全体个体计算概率, 其中 $F(x)$ 为适应度函数, 依据式(4)求得, fit_{max} 为种群中最大适应度, fit_{min} 为种群中最小适应度。

$$p_m(x) = \frac{fit_{max} - F(x)}{fit_{max} - fit_{min}} \quad (3)$$

依据该概率从种群中随机选取一个个体删除, 并重新初始化一个个体补充进该种群。为保证种群整体质量, 限制外来个体的适应度宜大于 0.4。

3.2 精度控制

提高目标识别精度是特征优选的最终目标, 通过 GA-SVM 耦合算法构建基于精度评价的适应度函数, 在收敛判断中引入种群重置机制逃离局部极小状态, 提高最终特征方案的识别精度。

3.2.1 适应度函数的构建

针对目标识别的要求, 根据训练样本集的识别误差和特征维数两个方面构建适应度函数:

$$F(x) = w_1 \times (1 - E_{漏分}(x) - E_{误分}(x)) + w_2 \times (1 - (d(x) - d_{min}) / (d_{max} - d_{min})) \quad (4)$$

式中, $E_{漏分}(x)$ 为训练样本集中漏分对象所占比重, $E_{误分}(x)$ 为错分对象所占比重。 $d(x)$ 为染色体 x 所包含特征的维数, d_{max} 为 x 可能包含的最大维数, d_{min} 为种群染色体中所含最小特征维数。 w_1 和 w_2 分别为目标识别精度和特征维数在适应度计算中所占权重, 满足 $w_1 + w_2 = 1$ 。

3.2.2 收敛条件和种群重置

算法中的收敛条件设置 3 种, 分别为: 种群中最佳个体的适应度大于 0.95, 且连续 5 代最佳个体的适应度没有改善; 种群中最佳个体的适应度大于 0.9, 且连续 10 代最佳个体的适应度没有改善; 算法已经进化了 100 代。

若连续 10 代种群中最佳个体的适应度没有改善, 且该适应度低于 0.9, 则认为算法陷入局部极小, 启动种群重置机制。保留种群中适应度最高的个体, 对其他个体, 根据个体的适应度随机保留, 利用初始化算法重置剩余个体, 再次启动遗传过程。

4 高分辨率遥感建筑物目标识别实验

4.1 实验数据和平台

实验选取某景覆盖武汉部分城区的 Quickbird 融合影像的两部分做建筑物识别, 影像的空间分辨率为 0.6m, 测试影像的大小分别为 1600×1600 以及

1200×800, 影像包含 4 个波段, 分别对应可见光蓝、绿、红波段和近红外波段。所用的实验平台为中国科学院遥感应用研究所开发的 SINCE2008。

4.2 特征提取

将测试影像用 MeanShift 方法在合适的尺度下进行分割, 实验选择影像在尺度上分别为 100(最小区域的大小为 100)与 200 时能够保证建筑物基元被较完整的分隔, 并且不与周边地物基元相混淆, 关于 MeanShift 方法的更多内容请参考相关文献 (Comaniciu & Meer, 2002)。利用其分割结果作为分类原数据, 分割结果分别包含对象 3236 个以及 1435 个(表 1)。从原数据中提取包含波谱特征、形状特征、纹理特征在内的 31 个特征。实验使用的 Quickbird 影像包含 4 个波段, 随着波段数目的增多, 可以适当增加几何特征的数量或提高权重以保证几何特征在最终识别中的贡献度。

表 1 特征列表

特征名	特征个数	
光谱特征	各波段亮度均值	4
	各波段亮度标准差	4
	小计	8
纹理特征	各波段 ASM	4
	各波段 IDM	4
	各波段 ENTROPY	4
	各波段 CONTRAST	4
	小计	16
几何特征	周长	1
	面积	1
	矩形宽	1
	矩形长	1
	矩形主方向	1
	形状指数	1
	紧凑度	1
	小计	7
总计	31	

光谱特征的计算简单。纹理特征是基于灰度-梯度共生矩阵提取的, 所提取的特征包括:

$$\text{逆差矩: IDM} = \sum_{i=0}^{n-1} \sum_{j=0}^{n-1} \frac{P_{ij}}{1+(i-j)^2}$$

$$\text{角二阶矩: ASM} = \sum_{i=0}^{n-1} \sum_{j=0}^{n-1} P_{ij}^2$$

$$\text{信息熵: Entropy} = \sum_{i=0}^{n-1} \sum_{j=0}^{n-1} P_{ij} \log P_{ij}$$

$$\text{对比度: Contrast} = \sum_{i=0}^{n-1} \sum_{j=0}^{n-1} (i-j)^2 P_{ij}$$

式中, P_{ij} 为共生矩阵 C 的第 (i, j) 个元素的值 C_{ij} 在灰度值为 i 梯度值为 j 处的共生矩阵的概率, 即 $P_{ij} = C_{ij} / \sum_i \sum_j C_{ij}$ 。另, 梯度图像是通过以下方法得

到: 中心像元与上下左右 4 个像元的差值求和, 再取绝对值。

主要的几何特征的计算方法如下:

$$\text{紧凑度: Compact} = 2 \times \sqrt{\pi \times \text{area}} / \text{perim}$$

$$\text{形状因子: ShapeIndex} = 0.25 \times \text{perim} / \sqrt{\text{area}}$$

式中, area 为对象面积, perim 为周长。

4.3 实验样本和参数说明

针对该遥感影像选择训练样本集和测试样本集(表 2)。训练样本集分为 4 类, 总计 276 个对象。测试样本集分为建筑及非建筑两类, 包含对象 537 个。

表 2 样本集

训练样本集		
类别名称	对象数量	
	影像 I	影像
建筑	67	78
阴影	63	34
绿地	77	87
路面	69	57
测试样本集		
类别名称	对象数量	
	影像 I	影像
建筑	123	110
非建筑	414	255

遗传算法参数设定如下: 种群规模为 50; 初始化时各染色体设置为 1 的概率为 0.3; 在适应度函数构建中, 本文认为最大限度提高识别精度是特征优选的最重要目标, 目标识别精度权重系数 W_1 设定为 0.9。

由于遗传算法具有遗传结果的不确定性, 而且相同特征子集, 不同排列顺序的特征向量对支持向量机的分类结果也有影响。实验用 GA-SVM 耦合的方法对相同的原数据进行 20 次实验, 将 20 次实验的平均结果作为评价 GA-SVM 耦合方法性能的依据。

SVM 算法采用三阶高斯核函数, simmoid 函数的 s 参数与 c 参数均为 1.0, epsilon-SVR 损失函数的 epsilon 值为 0.9, epsilon-SVR 的 c 参数值为 25, 训练结束门限值为 0.01。

4.4 比较方法及相关说明

使用以下几种方法进行特征优选并进行目标识别实验, 包括 PCA 特征降维方法、常规 GA 方法和经验方法等。在目标分类阶段, 这些对比方法均采用 SVM 分类器。PCA 特征降维时抽取若干个主成分, 这些主成分应表征 95% 以上的信息量。常规 GA 方法与本文方法的区别在于: 前者不采用个体优化选择机制、外来个体进入机制和种群重置机制。另外, 还选用最小距离分类器与 GA 耦合, 以比较该耦合方法与 GA-SVM 耦合方法的优劣。GA-SVM 耦合方法识别过程见图 2、图 3。

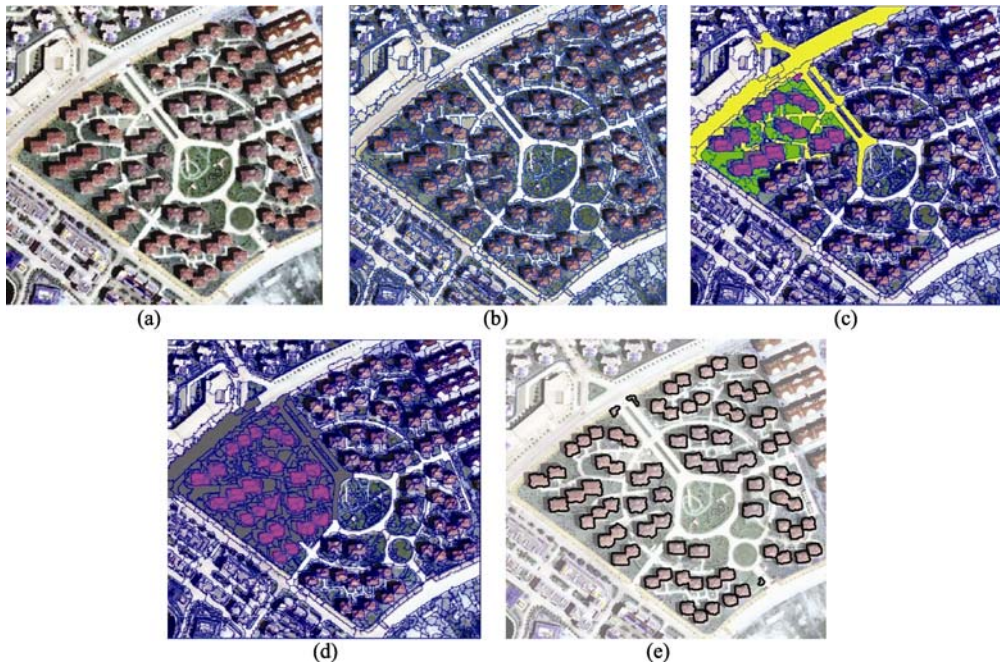


图2 使用 GA-SVM 耦合方法的建筑物识别过程()

(a) Quickbird 测试影像; (b) 多尺度分割结果; (c) 训练样本集; (d) 测试样本集; (e) 最优精度目标识别结果

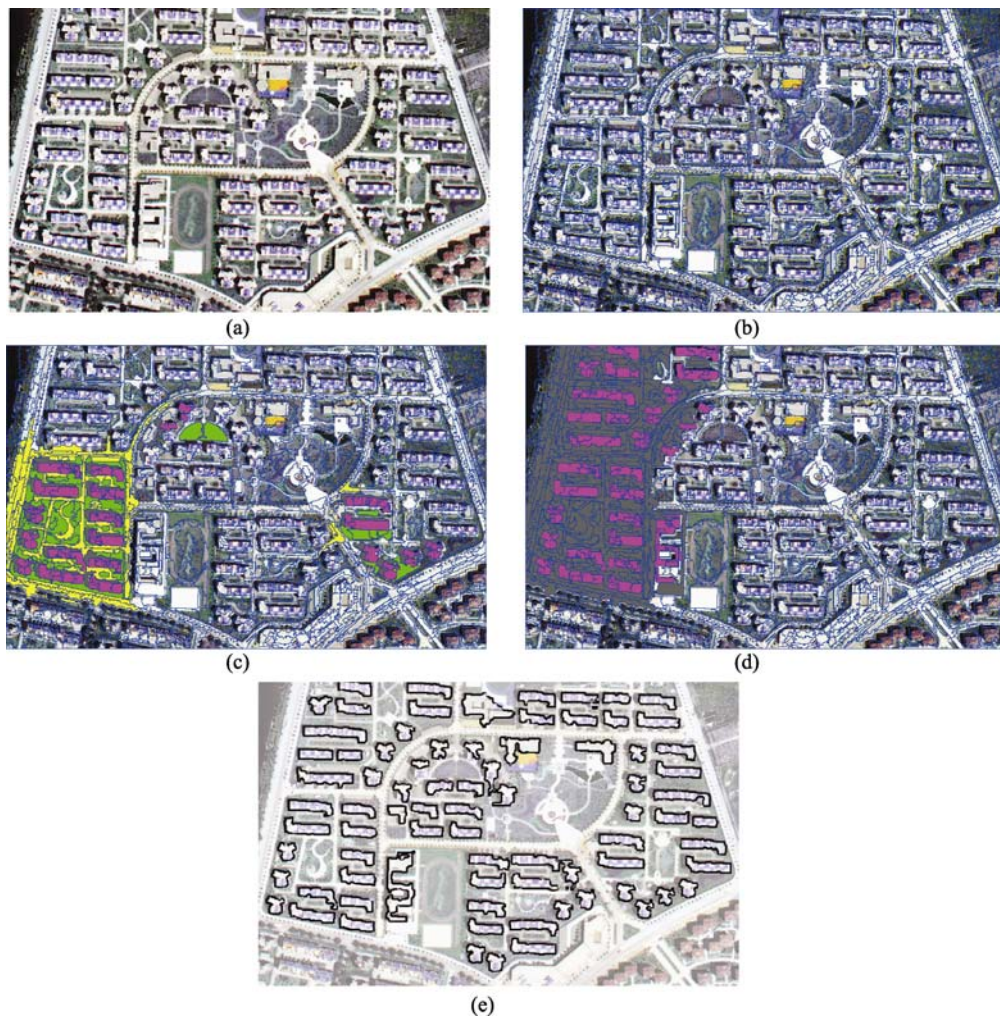


图3 使用 GA-SVM 耦合方法的建筑物识别过程()

(a) Quickbird 测试影像; (b) 多尺度分割结果; (c) 训练样本集; (d) 测试样本集; (e) 最优精度目标识别结果

4.5 实验结果与分析

实验结果显示(表 3、表 4), 使用 GA-SVM 耦合方法输出的最优特征子集平均包含的特征分别为 9.65 个和 8.25 个, 其中, 20 个输出子集均包含的特征有 6 个和 7 个(图 4(b)及图 5(b)), 最大识别精度为 98.48% 和 93.31%, 最小识别精度为 96.59% 和 90.66%, 平均精度为 97.86% 和 92.24%, 标准差为 0.41% 和 0.64%。这说明 GA-SVM 耦合方法在处理建筑物目标识别上具有较好的稳健性。优选特征结果见表 5 表 6。

将 GA-SVM 耦合后方法与常规建筑物目标识别的特征选择方法作比较, 结果如表 7。我们注意到, 当使用所有特征进行识别时, 识别精度最低, 仅为

50.76% 和 68.08%, 使用 PCA 降维后得到的最终识别精度略有提高, 由于未成熟收敛效应的存在, 并且实验所选区域光谱特征均较为明显, 常规 GA 与按经验仅使用光谱特征所得结果差别不大。对比各种方法发现, GA-SVM 耦合方法应用于建筑物目标识别后识别精度有明显的提高。通过与 GA 耦合最小距离分类器的分类结果的比较看出, 选择 SVM 作为耦合用分类器的优越性。与常规 GA 方法相比, 本文所提出的、耦合了改进的遗传算法和 SVM 的特征优选方法能保证 GA 的进化始终向提高目标识别精度的方向演进, 有效减低 GA 算法未成熟收敛的风险, 进而提高目标识别精度。同时, 优化后的结果可为同类遥感影像的识别提供借鉴。

表 3 测试影像 I 的 20 次实验的识别精度列表

实验序号	1	2	3	4	5	6	7	8	9	10
优选出特征数/个	11	9	9	12	12	11	10	8	9	8
分类精度/%	97.73	97.73	98.30	98.48	98.11	98.11	98.11	97.73	97.73	98.30
实验序号	11	12	13	14	15	16	17	18	19	20
优选出特征数/个	8	10	6	10	10	11	10	8	12	9
分类精度/%	97.54	98.30	96.59	97.54	97.54	97.54	98.11	97.73	98.11	97.92

表 4 测试影像 II 的 20 次优选结果列表

实验序号	1	2	3	4	5	6	7	8	9	10
优选出特征数/个	9	12	8	8	9	10	7	8	7	12
分类精度/%	93.03	92.68	92.61	92.20	93.17	92.13	91.99	91.50	93.17	93.31
实验序号	11	12	13	14	15	16	17	18	19	20
优选出特征数/个	6	7	9	9	6	9	10	4	8	7
分类精度/%	91.64	92.20	91.57	92.47	92.61	92.06	91.92	91.78	92.13	90.66

特征名称
平均亮度值_波段1
平均亮度值_波段2
平均亮度值_波段3
平均亮度值_波段4
面积
ASM_波段1
ASM_波段2
IDM_波段3
IDM_波段4
ENTROPY_波段1
ENTROPY_波段3
CONTRAST_波段3

(a)

特征名称
平均亮度值_波段1
平均亮度值_波段2
平均亮度值_波段3
平均亮度值_波段4
面积
ASM_波段1

(b)

特征名称
平均亮度值_波段1
平均亮度值_波段2
平均亮度值_波段3
平均亮度值_波段4
面积
ASM_波段1
ASM_波段2
IDM_波段3
IDM_波段4
ENTROPY_波段1
ENTROPY_波段3
CONTRAST_波段3

(a)

特征名称
平均亮度值_波段1
平均亮度值_波段2
平均亮度值_波段3
平均亮度值_波段4
面积
ASM_波段1

(b)

图 4 测试影像 的特征优选结果

(a) 最优精度下的优选结果; (b) 10 次以上优选结果均包含的特征

图 5 测试影像 的特征优选结果

(a) 最优精度下的优选结果; (b) 10 次以上优选结果均包含的特征

表 5 测试影像 I 的 20 次实验特征优选结果

实验编号	1	2	3	4	5	6	7	8	9	10	11	12	13	14	15	16	17	18	19	20
平均亮度值_波段 1																				
平均亮度值_波段 2																				
平均亮度值_波段 3																				
平均亮度值_波段 4																				
标准差_波段 1																				
标准差_波段 2																				
标准差_波段 3																				
标准差_波段 4																				
周长																				
面积																				
矩形宽																				
矩形长																				
矩形主方向																				
形状指数																				
紧凑度																				
ASM_波段 1																				
ASM_波段 2																				
ASM_波段 3																				
ASM_波段 4																				
IDM_波段 1																				
IDM_波段 2																				
IDM_波段 3																				
IDM_波段 4																				
ENTROPY_波段 1																				
ENTROPY_波段 2																				
ENTROPY_波段 3																				
ENTROPY_波段 4																				
CONTRAST_波段 1																				
CONTRAST_波段 2																				
CONTRAST_波段 3																				
CONTRAST_波段 4																				

表示特征包含在特征优选结果中

表 6 测试影像 II 的 20 次实验特征列表

实验编号	1	2	3	4	5	6	7	8	9	10	11	12	13	14	15	16	17	18	19	20
平均亮度值_波段 1																				
平均亮度值_波段 2																				
平均亮度值_波段 3																				
平均亮度值_波段 4																				
标准差_波段 1																				
标准差_波段 2																				
标准差_波段 3																				
标准差_波段 4																				
周长																				
面积																				
矩形宽																				
矩形长																				
矩形主方向																				
形状指数																				
紧凑度																				
ASM_波段 1																				
ASM_波段 2																				
ASM_波段 3																				
ASM_波段 4																				
IDM_波段 1																				
IDM_波段 2																				
IDM_波段 3																				
IDM_波段 4																				
ENTROPY_波段 1																				
ENTROPY_波段 2																				
ENTROPY_波段 3																				
ENTROPY_波段 4																				
CONTRAST_波段 1																				
CONTRAST_波段 2																				
CONTRAST_波段 3																				
CONTRAST_波段 4																				

表示特征包含在特征优选结果中

表 7 GA-SVM 耦合特征优选方法与其他优选方法的比较

特征选择方式	测试影像 I				测试影像			
	漏检	错检	错误率	正确率	漏检	错检	错误率	正确率
按经验仅使用光谱特征	3.03	9.85	12.88	87.12	3.76	6.97	10.73	89.27
使用全部特征	46.21	3.03	49.24	50.76	11.92	20.00	31.92	68.08
使用 PCA 降维	11.36	26.52	37.88	62.12	8.36	12.26	20.63	79.37
常规 GA 降维	3.03	11.36	14.39	85.61	2.72	6.62	9.34	90.66
使用 GA-SVM 耦合方法	0.00	1.52	1.52	98.48	2.72	3.97	6.69	93.31
使用 GA-最小距离分类器耦合方法	9.45	11.74	21.19	78.81	7.69	6.76	14.45	85.55

5 结论与讨论

提出了将 GA 中的特征降维和适应度函数构建与 SVM 中的特征空间映射、样本训练以及分类结果在内容上耦合后应用于高空间分辨率遥感影像目标识别的特征优选方法。实验结果表明,该方法能够有效降低特征空间维数,提高地物目标识别精度,同其他特征优选方法相比具有明显的优势。对遗传算法的改进能够改善未成熟收敛现象,获得更优化的遗传结果。对高分辨率遥感影像目标识别的特征选择有一定的参考价值。

需要指出的是,本文仅选用了 Quickbird 数据作为测试影像,且实验数据中建筑类型相对单一。如何提高 GA-SVM 方法的普适性,将该方法扩展应用到其他高分辨率数据及多种类型建筑物共存的影像数据中将是今后研究的重点。

REFERENCES

- Chen G L and Wang X F. 1999. Genetic Algorithm and Its Application. Beijing: Posts & Telecom Press
- Comaniciu D, Meer P. 2002. Mean shift: a robust approach toward feature space analysis. *IEEE Trans. on Pattern Analysis and Machine Intelligence*, **24**(5): 603—619
- He A X, Zhu Y H and An K. 2007. Tumor molecular classification based on genetic algorithms and support vector machines. *Journal of Data Acquisition & Processing*, **22**(1): 84—89
- Holland J H. 1973. Genetic algorithms and the optimal allocations of trials. *SIAM Journal of Computing*, **2**: 88—105
- Holland J H. 1975. Adaptation in Natural and Artificial System. Ann Arbor: The University of Michigan Press
- Li J M, Hu Y H and Chen X Q. 2006. Feature optimizing expert system for pattern recognition. *Electronics Optics&Control*,

13(1): 20—26

- Ming D P, Luo J C, Shen Z F, Wang M and Sheng H. 2005. Research on information extraction and target recognition from high resolution remote sensing image. *Science of Surveying and Mapping*, **30**(3): 18—20
- Niu L H and Ni G Q. 2005. Feature optimization for multi_sensor target recognition system. *Optical Technique*, **31**(3): 420—426
- Nello C and John S T. 2004. An Introduction to Support Vector Machines and Other Kernel-based Learning Methods. Cambridge: Cambridge University Press
- Vapnik V N. 1998. Statistical learning theory. New York: Wiley Interscience
- Xu J Q and Li G P. 2004. Feature selection for SVM based on genetic algorithm. *Computer Engineering*, **30**(24): 1—2, 182
- Zhang X H. 1997. Genetic algorithms and its application. *Fire Control & Command Control*, **22**(4): 49—53
- Zhang Y B and Zhang Q. 2005. Support vector machine for classification of remotely sensed image. *Geospatial Information*, **3**(4): 24—26

附中文参考文献

- 陈国良, 王煦法. 1999. 遗传算法及其应用. 北京: 人民邮电出版社
- 何爱香, 朱云华, 安凯. 2007. 基于遗传算法和支持向量机的肿瘤分子分类. *数据采集与处理*, **22**(1): 84—89
- 李军梅, 胡以华, 陈修桥. 2006. 模式识别的特征优化专家系统研究. *电光与控制*, **13**(1): 20—26
- 明冬萍, 骆剑承, 沈占锋, 汪闽, 盛昊. 2005. 高分辨率遥感影像信息提取与目标识别技术研究. *测绘科学*, **30**(3): 18—20
- 牛丽红, 倪国强. 2005. 多传感器目标识别系统的特征优化方法. *光学技术*, **31**(3): 420—426
- 许建强, 李高平. 2004. 基于遗传算法的支撑向量机的特征选取. *计算机工程*, **30**(24): 1—2, 182
- 章新华. 1997. 遗传算法及其应用. *火力与指挥控制*, **22**(4): 49—53
- 张耀波, 张迁. 2005. 基于 SVM 的遥感影像的分类. *地理空间信息*, **3**(4): 24—26